IX CONGRESSO BRASILEIRO DE ENGENHARIA E CIÊNCIAS TÉRMICAS
9th BRAZILIAN CONGRESS OF THERMAL ENGINEERING AND SCIENCES

Paper CIT02-0797

SIMULATION OF IRON COMBUSTION AT HIGH TEMPERATURE THROUGH A LIQUID OXIGEN JET

Rodrigo Ferreira Martins
Universidade do Vale do Paraíba – UNIVAP, Faculdade de Engenharia, Arquitetura e Urbanismo - FEAU
Av. Shishima Hifume, 2911 – São José dos Campos, SP –12.244-000

Humberto Araujo Machado
Universidade do Vale do Paraíba – UNIVAP, Instituto de Pesquisa e Desenvolvimento – IP&D
Av. Shishima Hifume, 2911 – São José dos Campos, SP –12.244-000
machado@univap.br

Abstract. *The reaction of iron combustion is an important chemical process in several engineering applications, yielding iron oxide and releasing energy. Such reaction is essential for the gas cutting of carbon steel plates, and can occur also in other devices where the ferrous stuff reaches high temperatures in a high oxygen concentration media. A basic aspect in such processes is to use the heat generated by the reaction to cut or heat the surface of the material. Usually, oxygen is provided as a gas, through a pre-heating flame. It was demonstrated that a micrometric droplet stream allows an excellent control of the droplet deposition over a surface. In this paper the impact of a liquid oxygen droplet jet is studied. The chemical and thermal processes that occur when the droplet jet impacts a steel flat plate are modeled and simulated, and the numerical results are compared with experimental data already available. The objective is to check if the reaction temperature rises over the iron melting temperature, determine the temperature and iron physical state during the reaction and verify if the reaction is able to sustain itself. Such knowledge would allow to estimate the possibility of the use of this process in oxi-cutting with some energy savings.*

Key words: *oxi-cutting , iron combustion, liquid oxygen.*

1. Introduction

Oxidation/combustion of iron at high temperature is an important chemical process in a range of technological applications an devices, yielding iron oxide (Fe_3O_4) and releasing energy (Kuo, 1986). Such reaction is essential in carbon steel cutting (Okomura e Taniguchi, 1982), and can be also observed in other processes where iron reaches high temperature inside medias with high concentration of oxygen, as some oxidation and propulsion equipments.

In the traditional cutting process, a heated oxygen-acetylene flame reacts with the iron, and the energy released by the exothermal reaction sustain the process. In this case, it is accepted that iron doesn't melt, as its melting point is over the ignition temperature. In fact, the heat responsible for cutting is that from the iron combustion, but a flame is needed to begin the reaction and keep the cutting zone heated behind the ignition temperature.

Poulikakos & Waldvogel (1997) have demonstrated that a micrometric droplet stream allows to an excellent control of droplet deposition over a surface, and applied this technique into welding of elements of electronic circuit boards. Such procedure would be applied to the cutting or welding of ferrous alloys through liquid oxygen droplets.

This investigates the combustion of iron with liquid oxygen droplets. The chemical and thermal processes which occurs when the droplets impact a low carbon steel flat plate are modeled, simulated and compared to some experimental data obtained from an simplified experimental set up. The objective is to verify if the processes of combustion occurs bellow the iron melting point, at which temperature the iron burns and if the reaction is self-sustainable.

2. Set up and analysis of experimental results

A droplet generator was built, which was made in two parts: in order to produce the LOX (liquid oxygen), a heat exchanger working via a counter flow of liquid nitrogen was used. The oxygen line was feed with gaseous oxygen at 8 bar. The droplet stream was generated through a pulse applied into a piezo-electric cylinder, which is crossed by the liquid flow of oxygen along its lenght. This perturbation causes the *Rayleigh Break up* of the liquid jet (Probstein, 1989), after it has left the tube, crossing a 50 μm safire orifice at its end. The small droplets were visualized through a stroboscope light coupled to the pulse generator. Figure (1) shows the droplet generator schematic. The size and frequency of the droplets may be changed according to the frequency of the pulse signal applied to the piezo-electric cylinder, as shown in Fig. (2). The approximate LOX mass flux obtained was 0.031 g/s.

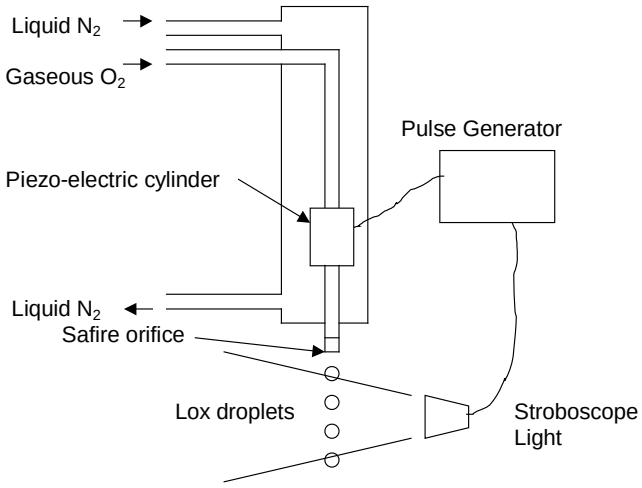

Figure 1. Droplet generator.

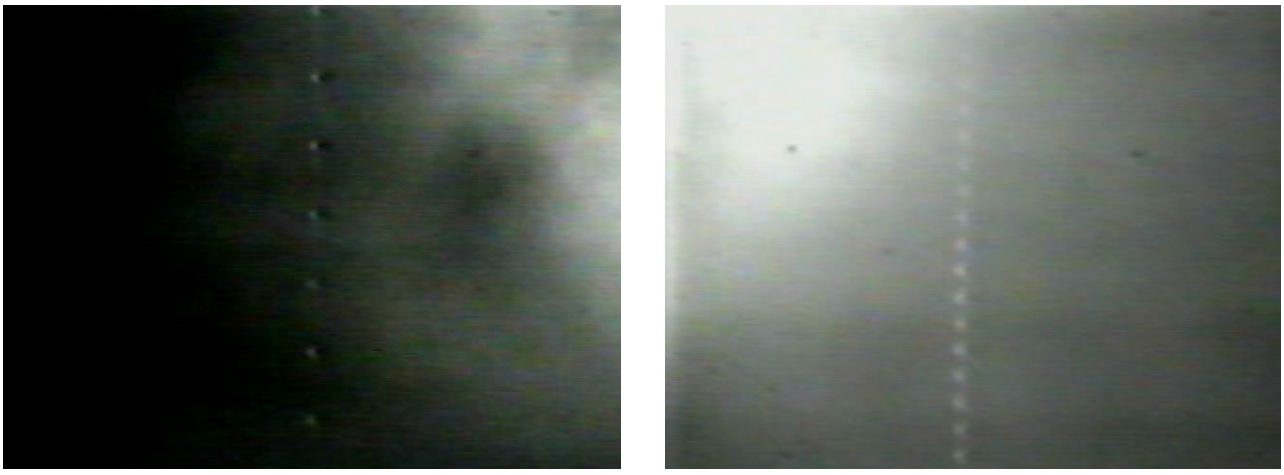

Figure 2. Frequency variation of LOX droplets.

During the test, the droplet stream impacts the surface of a flat plate of an hypoeutectic stainless steel *AISI No. C 1020* – chemical composition: 0.18-0.23 % C, 0.30-0.60 % Mn, 0.04 % max. P e 0.05 % max. S (Marks, 1958), heated by electrical resistance, through a 100 W electrical indutor. The smallest dimension of the test section warrants that the heating in this section would be the maximum, Fig. (3.a). A thermocouple type "B" was placed just bellow the point where droplets fell, Fig. (3.b), alowing to obtain temperature measurements with precision of 1 %.

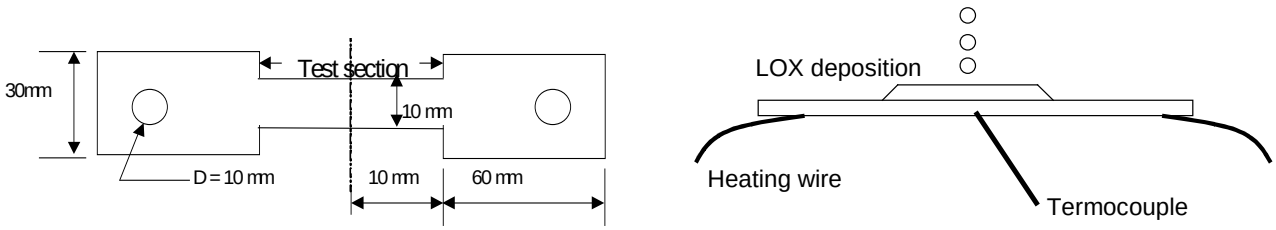

(a) Superior view (b) Lateral view

Figure 3. Test body (1 mm thick)

The experiment starts by adjusting the droplets frequency and size, Fig. (4). Figure (5) shows the evolution of the reaction. In Fig.(5.a), by the end of the pre-heating period, the plate is heated to red. In Fig.(5.b), reaction and cutting occurs. In Fig.(5.c) the plate was crossed by the stream and in Fig.(4.d) one can observe a hole, with some melted material placed around. The process is extremely fast and, even though yielding a small hole, the melting zone is much larger than the hole dimensions. It is considered that the reaction occurred only in the region crossed by the stream, but the melted material was scattered due the explosive velocity of reaction.

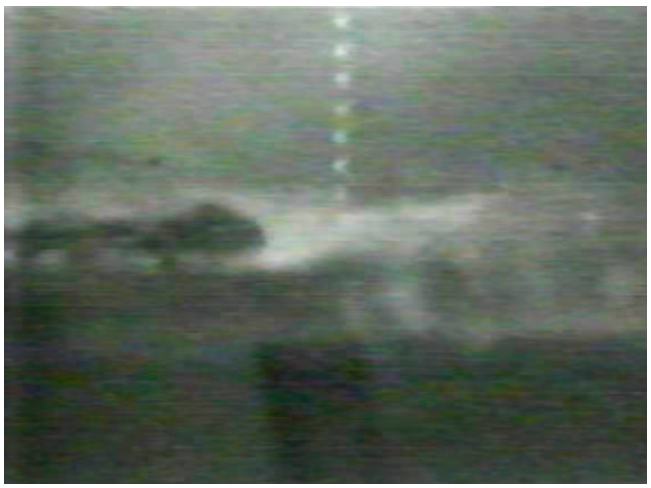

Figure 4. Droplet stream falling over the flat plate – thermocouple bellow.

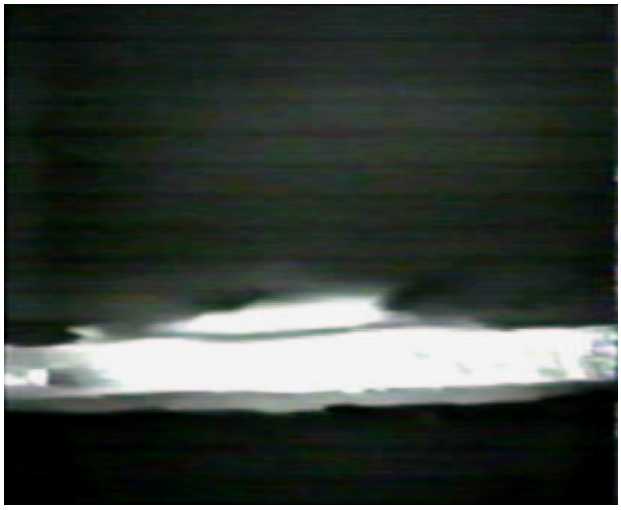

(a) Pré heating.

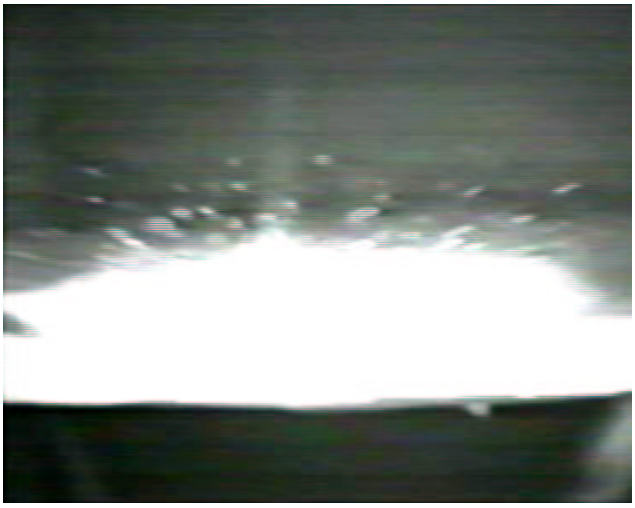

(b) Ignition and melting.

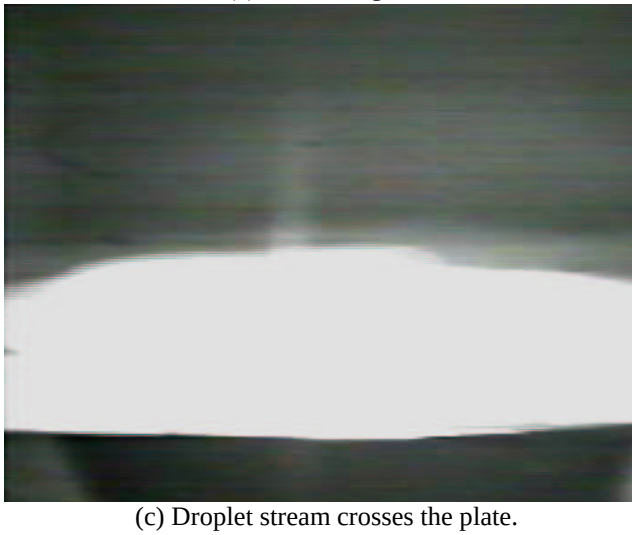

(c) Droplet stream crosses the plate.

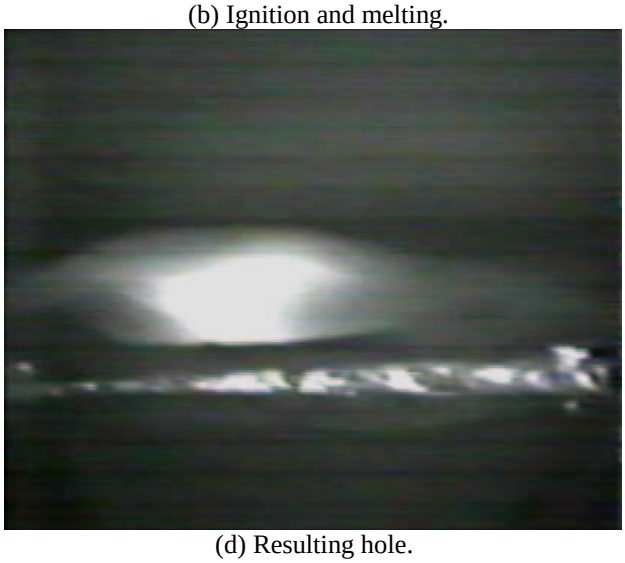

(d) Resulting hole.

Figure 5. Sequence of reaction afte pre-heating period.

Figure (6) shows the temperature profile measured by the thermocouple. The hole was yielded in the period where temperature stoped to raise. From Fig. (6), it is observed that fusion has begun at about 1000^{o} C. As the temperature was measured in a hotter region (inferior surface, where there is no LOX deposition – which is at -90^{o} C), it is supposed that melting started in a lower temperature. Ignition temperature usually accepted is 870^{o} C (White Martins, 2000).

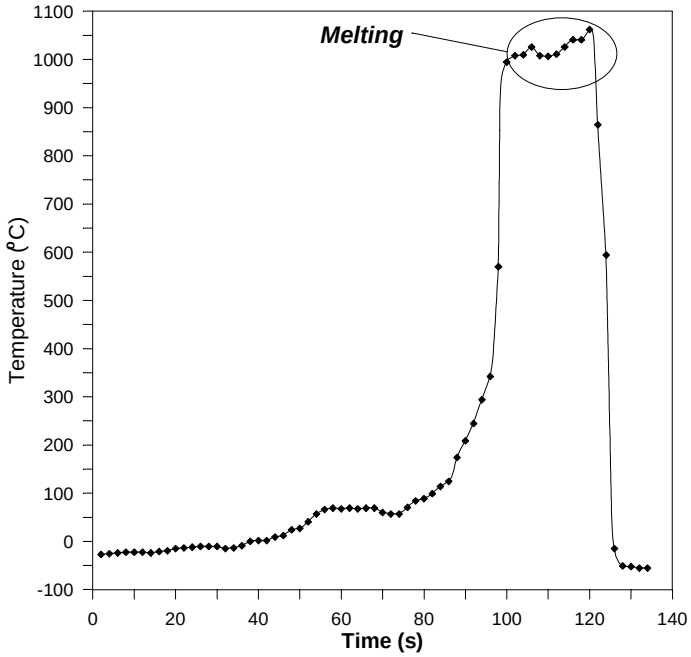

Figure 6. Temperature measured by thermocouple.

3. Mathematical model

The species of iron oxide produced during the combustion and the heat released are (Alberty e Silbey, 1996):

$$Fe + 0{,}5\ O_2 = FeO + 64{,}3 \text{ kcal/g mol} \quad (1)$$

$$3Fe + 2\ O_2 = Fe_3O_4 + 266{,}9 \text{ kcal/g mol} \quad (2)$$

$$2Fe + 1{,}5\ O_2 = Fe_2O_3 + 198{,}5 \text{ kcal/g mol} \quad (3)$$

There is a strong doubt concerning the proportion of material among each oxide produced. Due to the proximity between reactions, given by Eq. (2) and (3) , and the high proportion they take in the process, it can be simplified considering only reaction (2), in only one step (Glizmanenko, 1962; Rossi, 1954). The rate of reaction is supposed to have na Arhenius behavior (Russel, 1980; Kuo, 1986), and the reaction is considered to be bi-molecular of 1st order, with the iron in the solid state (Kuo, 1986):

$$\frac{dC_{Fe}}{dt} = -K(T)C_{o_2} \quad (4)$$

C_{Fe} - concentration of iron (moles/m^3)
C_{O2} - concentration of molecular oxygen (moles/m^3)
K(T) - constant of reaction, function of temperature (mol_{Fe}/mol_{O2}.s)

Observing Fig. (5), one can suppose that the hole is done over a region covered by LOX. Reaction starts over such deposit and becomes a melting zone in that region. However, the pressure wave caused by the exothermic reaction expels the excess of LOX and melted oxides, and probably some melted iron not reacted too. The reaction is kept running through the LOX supplied by the jet, filling an area equivalent to the droplets diameter (100 μm – the safire orifice has half of this diameter, but the formation of droplets results in an expansion of the diameter - Poulikakos and Waldvogel, 1997).

In the conventional oxy-cutting process, the oxygen diffuses through the oxide layer in the wall of the melting orifice (*kerf*), playing an important role in the reaction. In the specific case studied here, the oxygen diffusion will be neglected due the velocity of the reaction.

The mathematical model is developed from a integral formulation applied to a control volume, which obeys the basic assumptions of oxy-cutting, as summarized by Davies (1993). The process was divided in two parts: pre-heating and combustion. The two different control volumes used are showed in Fig. (7). The reaction zone is assumed to be continuously fed with LOX, until the oxygen concentration reaches 100 %. As all the oxide produced is expelled from the control volume, the final concentration of iron at the end will be 0 %.

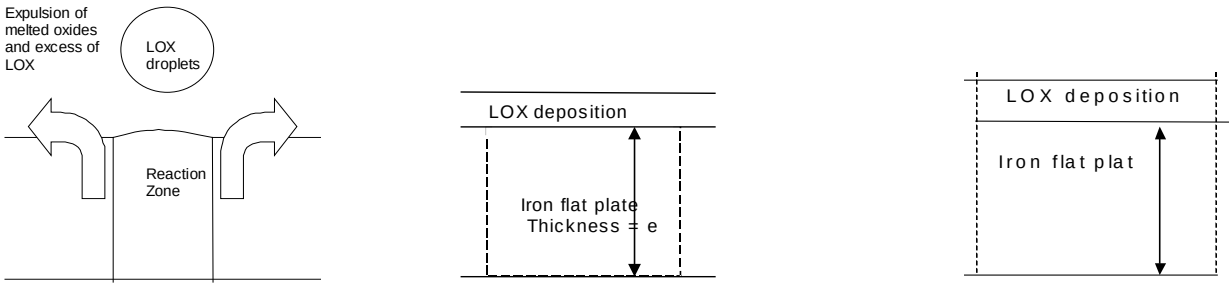

(a) Schematic view *(b) V.C. Pre-heating* *(c)V.C. Oxidation*

Figure 7. Control volumes used in each part of the process.

During the pre-heating the mass transport is neglected. The mass conservation during the reaction, supposing constant properties and homogeneous inputs and outputs is given as:

$$\frac{dm}{dt} = \dot{m}_{Fe_3O_4} - \dot{m}_{LOX} \tag{5}$$

where $\dot{m}_{Fe_3O_4}$ e $\dot{m}_{LOX}$ are the mass flux for the oxide and for the LOX supplied, respectively, obtained from the rate of reaction, m is the total amount of mass within the control volume V, showed in Fig. (7.b), at any instant. The necessary LOX mass flux to feed the reaction will be:

$$\dot{m}_{LOX} = V.M_{O_2}\left(\frac{dC_{O_2}}{dt} + 2\frac{dC_{Fe_3O_4}}{dt}\right) \tag{6}$$

where M is the molar mass of for each specie. In this model, at any moment the concentration of oxide is zero, because all oxide is expulsed at the instant of its formation. However, the rate of formation (which is the time derivative of the concentration) is not null.

The conservation of energy during the pré-heating is:

$$\rho_{Fe}.Cp_{Fe}\frac{dT}{dt} = \frac{\dot{Q}}{V} \tag{7}$$

where $\dot{Q}$ is the heat changed among the control volume and the environment, in Watts:

$$\frac{\dot{Q}}{V} = q_e + q_{conv} + q_{cond} + q_{rad} + q_{LOX} \tag{8}$$

q_e is the heat flux generated by Joule effect (electrical resistance) per volume unit (W/m^3)
q_{conv} = is the heat flux lost by convection for the air, at 25^o C.

$$q_{conv}. = h_\infty .e.(T_\infty - T) \tag{9}$$

where h_∞ is the film coefficient, obtained according Özisik (1990) and T_{oo} is the mean environment temperature.
q_{cond} is the heat flux lost by conduction through the interior of the plate, which will be neglected due the high thermal conductivity of the metal.
q_{rad} is the heat flux lost by thermal radiation:

$$q_{rad} = \sigma.\varepsilon.e(T_\infty{}^4 - T^4) \tag{10}$$

where σ is the Stephan-Botzman Constant (σ=5.67 x 10^{-8} $W/m^2.k^4$) and ε is the iron emisivity.
q_{LOX} is the heat flux absorbed by the LOX that evaporates over the superior surface of the flat plate. Considering that the change is equilibrated all time over the whole surface:

$$q_{LOX} = \dot{m}_{LOX\ droplets}.H_{lv} \tag{11}$$

During the combustion, LOX and iron are considered an homogeneous mixture within the reaction zone. The energy balance yields:

$$\frac{1}{V}\frac{dH}{dt} = \frac{\dot{Q}}{V} + \frac{\dot{m}_{Fe_3O_4}}{V}.h_{Fe_3O_4} - \frac{\dot{m}_{LOX}}{V}.h_{LOX} \tag{12}$$

where h is the enthalpy of each specie, in J/kg, and H is the total enthalpy of the mixture inside the control volume:

$$\begin{aligned} H &= m_{Fe}h_{Fe}(T) + m_{O_2}h_{O_2}(T) + m_{Fe_3O_4}h_{Fe_3O_4}(T) = \\ &V.M_{Fe}.C_{Fe}h_{Fe}(T) + V.M_{O_2}.C_{O_2}h_{LOX} + V.M_{Fe_3O_4}.C_{Fe_3O_4}h_{Fe_3O_4}(T) \end{aligned} \tag{13}$$

In this case, it is assumed that $C_{Fe_3O_4} = 0$ and the oxygen is kept in the liquid phase at saturation condition (with constant enthalpy), and the oxide produced is expulsed at melting temperature. Since all components are in solid or liquid states, pressure and specific volume inside control volume are constants, and enthalpy is considered equal to internal energy. Such approximation may be extended for the case of gaseous oxygen, as combustion occurs in contact to the environment and in this case the amount of oxygen is much smaller than for the LOX case.

Taking the derivative of Eq. (13) in time and replacing the result in Eq. (12), appears:

$$\begin{aligned} &M_{Fe}.C_{Fe}.\frac{dh_{Fe}}{dt} + M_{Fe}.h_{Fe}(T).\frac{dC_{Fe}}{dt} + M_{O_2}.h_{LOX}.\frac{dC_{O_2}}{dt} \\ &+ M_{Fe_3O_4}.h_{Fe_3O_4}(T).\frac{dC_{Fe_3O_4}}{dt} = \frac{\dot{Q}}{V} + \frac{\dot{m}_{Fe_3O_4}}{V}.h_{Fe_3O_4} - \frac{\dot{m}_{LOX}}{V}.h_{LOX} \end{aligned} \tag{14}$$

The terms of $\dot{Q}$ for the reaction have to be modified:
q_e – as ignition temperature was reached, electric heating is turned off.
q_{LOX} – this term is taking into account in the input of LOX, Eq. (12).
q_q – is the heat of reaction, in W/m^3, to be added to the others terms, given as:

$$q_q = \Delta h_f.M_{O_2}.\frac{dC_{Fe_3O_4}}{dt} \tag{15}$$

The specific enthalpy of LOX is the liquid saturated enthalpy at 1 atm. The enthalpy of the other reagents are:

$$h_{Fe} = cp_{Fe\text{-}L}(T - T_{melting}) + cp_{Fe\text{-}S}(T - T_\infty) + H_{sl\text{-}Fe} \tag{16}$$

$$h_{O_2} = h_{LOX} = cp_{O_2\text{-}G}(T_{sat} - T_\infty) + H_{lv\text{-}O_2} \tag{17}$$

$$h_{Fe_3O_4} = cp_{Fe_3O_4\text{-}L}(T - T_{melting}) + cp_{Fe_3O_4\text{-}S}(T - T_\infty) + H_{sl\text{-}Fe_3O_4} \tag{18}$$

where H_{lv} e H_{sl} are the latent heats of evaporation and melting of each substance, respectively.

The variation of temperature and phase change must be considered for the determination for the enthalpy of formation of the oxide - Δh_f, expressed as:

$$0{,}724.(Fe_{(T)} - h_{Fe}) + 0{,}276.(O_{2(T,L)} - h_{O_2}) \rightarrow Fe_3O_{4(T)} - h_{Fe_3O_4} + \Delta h_f^o \tag{19}$$

$$\Delta h_f(T) = \Delta h_f^o(T) - h_{Fe_3O_4}(T) + 0{,}724.h_{Fe}(T) + 0{,}276.h_{O_2}(T) \tag{20}$$

where $\Delta h_f^o = 4{,}83 \times 10^6$ J/kg is the standard enthalpy of formation of the oxide.

4. Numerical solution

During the pre-heating, the model is validated comparing the theoretical value of the electrical energy input with the experimental one. As the temperature profile is known, it is possible to find analytical functions for T(t) and dT/dt, what allows to obtain $q_e(t)$.

The chemical reaction is simulated via a system of ordinary differential equations:

$$\frac{dC_{Fe}}{dt} = -K(T)C_{o_2} \tag{21}$$

$$\frac{dC_{Fe_3O_4}}{dt} = -\frac{1}{3}\frac{dC_{Fe}}{dt} \tag{22}$$

$$\frac{dC_{O_2}}{dt} = -\frac{\rho_{O_2}}{M_{O_2}}\frac{M_{Fe}}{\rho_{Fe}}\frac{dC_{Fe}}{dt} \tag{23}$$

$$\frac{dh_{Fe}}{dt} = \left[-M_{Fe}.h_{Fe}(T).\frac{dC_{Fe}}{dt} - M_{O_2}.h_{O_2}(T).\frac{dC_{O_2}}{dt} - M_{Fe_3O_4}.h_{Fe_3O_4}(T).\frac{dC_{Fe_3O_4}}{dt} + \frac{\dot{Q}}{V} - \frac{\dot{m}_{Fe_3O_4}}{V}.h_{Fe_3O_4}(T) + \frac{\dot{m}_{LOX}}{V}.h_{LOX} \right] / (M_{Fe}.C_{Fe}) \tag{24}$$

$$\frac{dT}{dt} = \begin{cases} \frac{1}{Cp_{Fe}}\frac{dh_{Fe}}{dt} & \text{if } T \neq T_{melting\ Fe} \\ 0 & \text{if } T = T_{melting\ Fe} \end{cases} \tag{25}$$

The computational program was built in FORTRAN, and the numerical solution was done via the routine DIVPAG, from the IMSL library (1989), through the GEAR method for initial value problems. The initial conditions are:

$$C_{Fe}(0) = m_{Fe}(0).M_{Fe}/V \tag{26}$$

$$C_{O_2}(0) = m_{O_2}(0).\ M_{O_2}/V \tag{27}$$

$$C_{Fe_3O_4}\ (0) = 0 \tag{28}$$

$$H_{Fe}(0) = Cp_{Fe\text{-}s}.[\ T(0) - T_{\infty}\ ] \tag{29}$$

$$T(0) = 870^{o}\ C \text{ (ignition temperature for iron combustion)} \tag{30}$$

The initial volume is obtained from the control volume showed in Fig. (7). The thickness of the LOX deposition is estimated from the equilibrium among the hydrostatic pressure and the surface tension (2,3 mm), added to the flat plate thickness, resulting in a height of 3,3 mm. Initial concentrations are:

$$C_{Fe}(0) = \frac{m_{Fe}(0)}{V}.M_{Fe} = \rho_{Fe}.\frac{A.e}{A..h}.M_{Fe} = \rho_{Fe}.\frac{e}{h}.M_{Fe} \tag{31}$$

$$C_{O_2}(0) = \frac{m_{O_2}(0)}{V}.M_{O_2} = \rho_{O_2}.\frac{A.(h-e)}{A..h}.M_{O_2} = \rho_{Fe}.\frac{(h-e)}{h}.M_{Fe} \tag{32}$$

Properties of oxygen, iron and Fe_3O_4 were obtained from literature data (respectively: Lide, 1980, Walker and Tam, 1991, Alberty and Silbey, 1996). Due the absence of data in literature, a mean value for K was estimated from experimental data of Steinberg et al (1992, 1998), considering the temperature constant and equal to the ignition temperature (870^{o} C). Although this approximation, the value used (K = 425,29 $mol_{Fe}/mol_{O2}.s$) may be considered representative for this process.

5. Results

5.1. Validation of the mathematical model – pre-heating

From the curve T x t, Fig. (7), an analytical function was adjusted for the temperature variation:

$$T(t) = 0{,}0337008.\ e^{0.100274.t} \tag{33}$$

Applying Eq.(33) in Eq.(7), it was possible to obtain curves for each factor of heating/cooling in the test section, that is showed in Fig. (8.a). The fraction of each loss compared to the electrical heat input is showed in Fig. (8.b). As the test section approaches to the ignition temperature, their importance vanish and they become negligible. If the final volumetric input of electrical energy is multiplied for the total volume of the control volume, the mean heating power is found equal to 66 W, what is coherent with the physical process and the induction power (100 W).

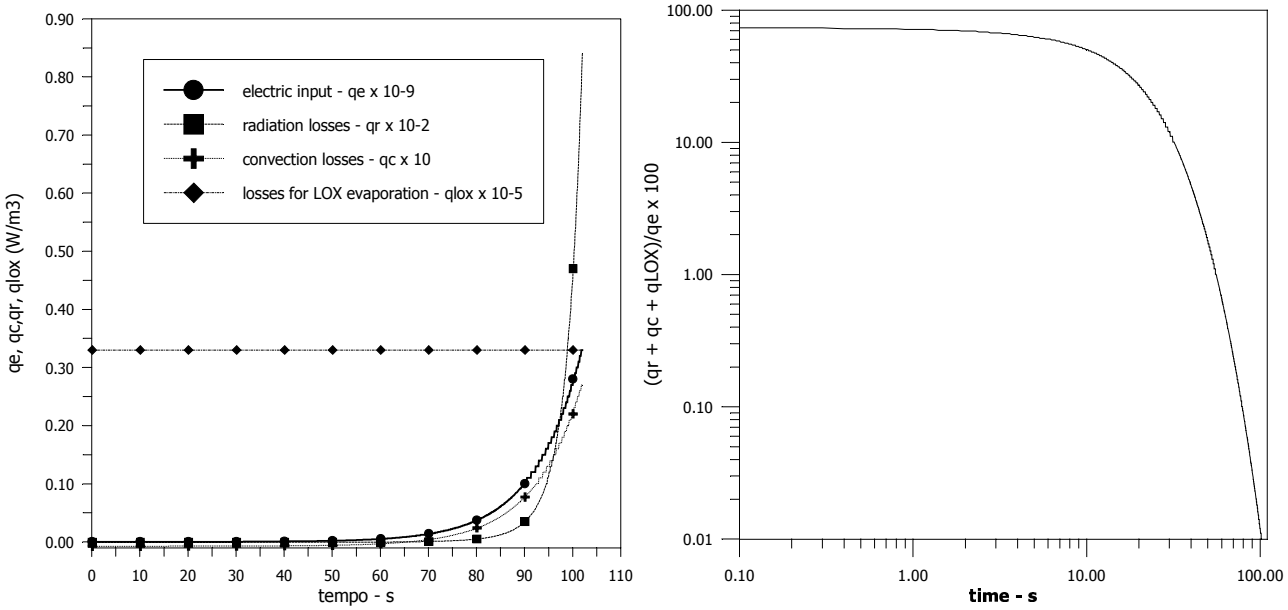

a) Variation of the effective heat input and the losses *b) Heat losses as fractions of the electrical input*

Figure 8. Electrical heat input and heat losses during pre-heating.

5.2. Combustion

The mathematical model was applied to iron combustion with Liquid oxygen (LOX) at saturation condition and gaseous oxygen (GOX) at atmospheric pressure. The gaseous oxygen releases more energy, due to its higher enthalpy, what contributes to increase the heat of reaction, as showed in fig. (9.a). The final temperature was also higher with the GOX – Fig. (9.b), but the maximum temperature was reached faster by the use of LOX, what indicates a higher heating power.

Considering the same initial concentration, the rate of reaction for LOX was much higher, due to the difference of density, allowing to obtain a higher concentration of O_2 inside the reaction zone, as shown in Fig. (10), resulting in a strong impact over the reaction rate.

In both cases, the final temperature is behind the dissociation temperature of the oxide (2257^o C), and the evaporation temperature of the iron (3133^o C). This fact would reduce the value of the highest temperature to one of this values. As a consequence, the Glassman hypothesis (as cited by Steinberg et al, 1992) – that admits the reaction occurs with iron in solid state – does not correspond to the results of the model. According to the results, the reaction occurs with the iron in liquid state, in agreement with to the results presented by Steinberg et al (1992).

The final results for each oxygen phase employed, taking the percentages relative to a GOX base, are shown in Table (1), and indicates that, although the LOX release only 24 % of the heat distributed in the test section and the maximum temperature be 37.3 % less, the reaction time reduces 74.8 %, and the oxide enthalpy fall only 20.9 %, what confirms that the reaction is self-sustainable.

Table 1. Results for the end of reaction

parameter	LOX	GOX	Variation %
Reaction time (s)	0,0033634	0,013357	-74,8
Final Temperature (^{o}C)	2.267,4	3615,9	-37,3
Final oxide enthalpy (J/kg)	2,23 x 10^6	2,82 x 10^6	-20,9
Energy output from test section (1) (J)	1.474,9	6.146,8	-76,0

(1) Heat transported by the oxide from the test section at the end of reaction.

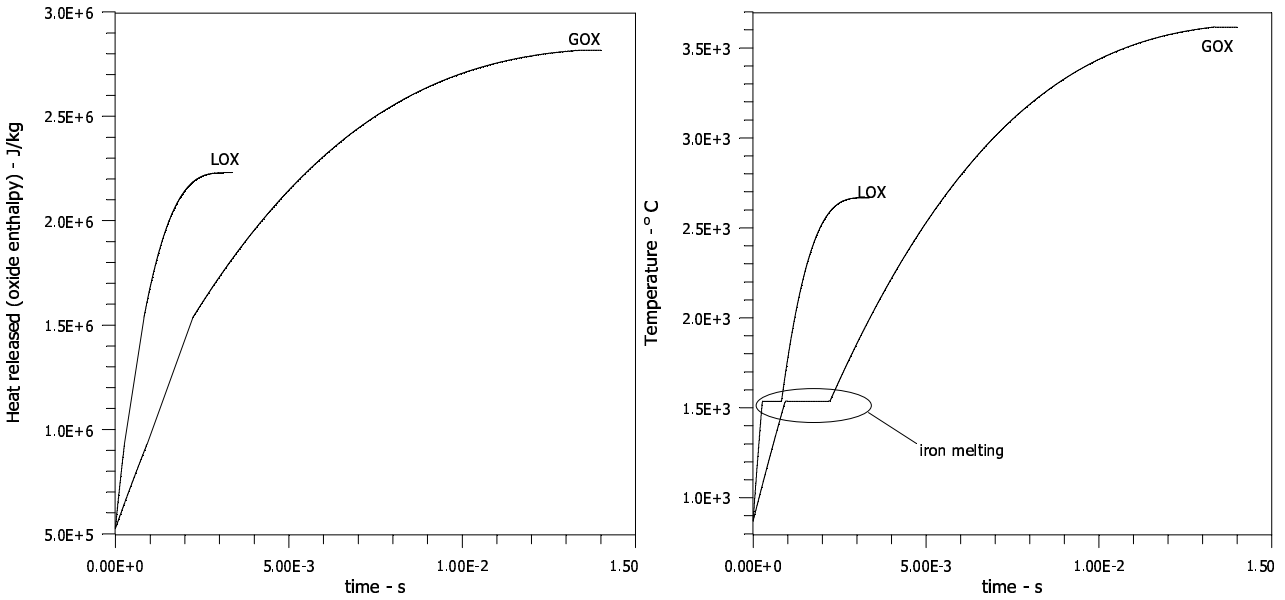

a) Oxide enthalpy x time *b) Temperature x time*

Figure 9. Results for energy balance in the reaction zone.

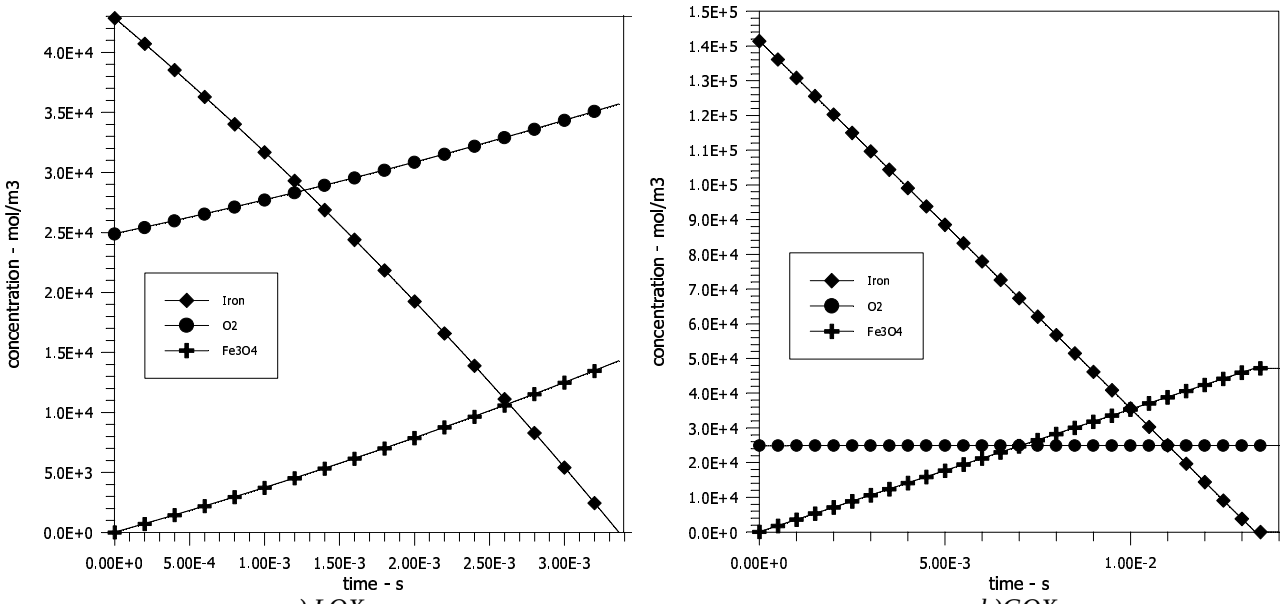

a) LOX *b)GOX*

Figure 10. Concentration x time in the reaction zone.

6. Conclusions

In this work the reaction of iron combustion was simulated with oxygen in the liquid phase. The model was validated through the comparison of experimental and theoretical data and the results for the reaction via a LOX droplet stream over an iron flat plate were compared with that for the use of GOX.

It was verified that the reaction rate is quite accelerated due the use of saturated liquid oxygen. According to the results, the iron and the oxide reacts in the liquid state, confirming recent studies that opposes to the traditional hypothesis the iron keeps in the solid state during the reaction. The processes has showed to be self-sustainable, although producing less energy then the gaseous oxygen. With respect to further research, it is proposed a more detailed mathematical model, taking into account the movement of the fluids, the absence of chemical equilibrium and the presence of alloy elements and impurities, and the study of economical viability of the use of LOX in steel cutting.

7. Acknowledgements

The authors would like to acknowledge CAPES and FAPESP for the financial support.

8. References

Alberty, R. A., Silbey , R .J., 1996, "Phisical Chemistry", 2nd Editon, Jonh Wiley & Sons, Inc.USA.
Davies, A. C., 1993, "Welding Science and Technology", Vol. 2, Cambridge University, NY.
Glizmanenko, D., Yevseyev, G., 1962, "Gas Welding and Cutting", Mir Publishers, Moscow.
Kuo, K. K., 1986, "Principles of Combustion", Wiley-Interscience, NY.
Lide, D. R. ,1990-1991, "Handbookk of Chemistry and Physics", 71st Edition ,CRC Press, USA.
Marks, L. S. (Ed.), 1958, "Mechanical Engineer's Handbook", McGraw-Hill, NY
Okomura, T., Taniguchi, C., 1982, "Engenharia de Soldagem e Aplicações", Rio de Janeiro.
Özisik, N. M., 1990, "Transferência de Calor", Editora Guanabara, Rio de Janeiro.
Poulikakos, D., Waldvogel, J. M., 1997, "Solidification Phenomena in Picoliter Size Solder Droplet deposition on a Composite Substrate', Int. J. Heat & Mass Transfer, Vol. 40, No. 2, pp 295-309.
Probstein, R. F., "Physical Chemical Hydrodynamics – An Introduction", Butterworths, USA, 1989.
Rossi, B. E., 1954, "Welding Engineering", McGraw-Hill Book Company, INC. USA.
Russel, J.B., 1980, "Química Geral", McGraw-Hill do Brasil ltda. São Paulo.
Steinberg, T. A., Mulholland, G. P., Wilson, D. B., 1992, "The Combustion of Iron in High-Pressure Oxygen, Combustion and Flame", Vol. 89, pp 221-228.
Steinberg, T. A., Kurtz, J., Wilson, D. B., 1996, "The Solubility of Oxygen in Liquid Iron Oxide During the Combustion of Iron Rods in High–Pressure Oxygen", Combustion and Flame, Vol. 113, pp 27-37.
Walker, P. e Tarn ,W. H., 1991, "HandBook of Metal Etchants", CRC Press, Florida.
White Martins, 2000, "Catalogs and Manuals of Welding and Cutting", Brazil.